11748 *Inorg. Chem.* **2009**, *48*, 11748–11754
DOI: 10.1021/ic901807k

Inorganic Chemistry
Article

Two-Dimensional Networks of Lanthanide Cubane-Shaped Dumbbells

Didier Savard,[†] Po-Heng Lin,[†] Tara J. Burchell,[†] Ilia Korobkov,[†] Wolfgang Wernsdorfer,[‡] Rodolphe Clérac,[§,∥] and Muralee Murugesu*[,†]

[†]*Chemistry Department, University of Ottawa, 10 Marie Curie, Ottawa, Canada, K1N 6N5,* [‡]*Institut Néel, National Center for Scientific Research* (*CNRS*) *Nanosciences Department, BP 166 25 Avenue des Martyrs, 38042, Grenoble, France,* [§]*CNRS, UPR 8641, Centre de Recherche Paul Pascal* (*CRPP*), *115 Avenue du Dr. Albert Schweitzer, Pessac, F-33600, France, and* [∥]*Université de Bordeaux, UPR 8641, Pessac, F-33600, France*

Received September 10, 2009

The syntheses, structures, and magnetic properties are reported for three new lanthanide complexes, $[Ln^{III}_4(\mu_3-OH)_2(\mu_3-O)_2(cpt)_6(MeOH)_6(H_2O)]_2$ (Ln = Dy (**1**·15MeOH), Ho (**2**·14MeOH), and Tb (**3**·18MeOH)), based on 4-(4-carboxyphenyl)-1,2,4-triazole ligand (Hcpt). The three complexes were confirmed to be isomorphous by infrared spectroscopy and single-crystal X-ray diffraction. The crystal structure of **1** reveals that the eight-coordinate metal centers are organized in two cubane-shaped moieties composed of four Dy^{III} ions each. All metal centers in the cubane core are bridged by two μ_3-oxide and two μ_3-hydroxide asymmetrical units. Moreover, each cubane is linked to its neighbor by two externally coordinating ligands, forming the dumbbell $\{Dy^{III}_4\}_2$ moiety. Electrostatic interactions between the ligands of the triazole-bridged dimers form an extended supramolecular two-dimensional arrangement analogous to a metal-organic framework with quadrilateral spaces occupied by ligands from axial sheets and by four solvent molecules. The magnetic properties of the three compounds have been investigated using dc and ac susceptibility measurements. For **1**, the static and dynamic data corroborate the fact that the $\{Dy^{III}_4\}$ cubane-shaped core exhibits slow relaxation of its magnetization below 5 K associated with a single-molecule magnet behavior.

Introduction

The science of organizing molecules in a predetermined multidimensional environment by using intermolecular interactions, commonly known as supramolecular chemistry, is the main subject of a growing scientific interest.[1] In the past decade, this methodology gave birth to fascinating novel areas of research including rotaxanes,[2] building blocks,[3] host−guest

*Fax: (613) 562 5170. Telephone: (613) 562 5800 ext. 2733. E-mail: m.murugesu@uottawa.ca.

(1) (a) Lehn, J.-M. *Supramolecular Chemistry: Concepts and Perspectives*; VCH: Weinheim, Germany, 1995.(b) Diederich, F. *Angew. Chem., Int. Ed.* **2007**, *46*, 68 and references cited therein. (c) Pitt, M. A.; Johnson, D. W. *Chem. Soc. Rev.* **2007**, *36*, 1441. (d) Fabbrizzi, L.; Poggi, A. *Chem. Soc. Rev.* **1995**, *24*, 197. (e) Kudernac, T.; Lei, S.; Elemans, J. A. A. W.; Feyter, S. D. *Chem. Soc. Rev.* **2009**, *38*, 402. (f) Steed, J. W.; Atwood, J. L. *Supramolecular Chemistry*; John Wiley and Sons: New York, 2009. (g) Lehn, J.-M. *Science* **1993**, *260*, 1762. (h) Oshovsky, G. V.; Reinhoudt, D. N.; Verboom, W. *Angew. Chem., Int. Ed.* **2007**, *46*, 2366.

(2) (a) Balzani, V.; Credi, A.; Venturi, M. *Chem. Soc. Rev.* **2009**, *38*, 1542. (b) Faiz, J. A.; Heitz, V.; Sauvage, J.-P. *Chem. Soc. Rev.* **2009**, *38*, 422. (c) Loeb, S. J. *Chem. Soc. Rev.* **2007**, *36*, 226. (d) Champin, B.; Mobian, P.; Sauvage, J.-P. *Chem. Soc. Rev.* **2007**, *36*, 358. (e) Tian, H.; Wang, Q.-C. *Chem. Soc. Rev.* **2006**, *35*, 361.

(3) (a) Davis, J. T.; Spada, G. P. *Chem. Soc. Rev.* **2007**, *36*, 296. (b) Toma, L. M.; Lescouëzec, R.; Pasán, J.; Ruiz-Pérez, C.; Vaissermann, J.; Cano, J.; Carrasco, R.; Wernsdorfer, W.; Lloret, F.; Julve, M. *J. Am. Chem. Soc.* **2006**, *128*, 4842. (c) Würthner, F.; Sautter, A.; Thalacker, C. *Angew. Chem., Int. Ed.* **2000**, *39*, 1243. (d) Nielsen, M. B.; Lomholt, C.; Becher, J. *Chem. Soc. Rev.* **2000**, *29*, 153. (e) Gómez, R.; Seoane, C.; Segura, J. L. *Chem. Soc. Rev.* **2007**, *36*, 1305. (f) Perry, J. J.; Perman, J. A.; Zaworotko, M. J. *Chem. Soc. Rev.* **2009**, *38*, 1400.

(4) (a) Organo, V. G.; Rudkevich, D. M. *Chem. Commun.* **2007**, 3891. (b) Bauer, R. E.; Clark, C. G., Jr.; Müllen, K. *New J. Chem.* **2007**, *31*, 1275. (c) Petitjean, A.; Khoury, R. G.; Kyritsakas, N.; Lehn, J.-M. *J. Am. Chem. Soc.* **2004**, *126*, 6637. (d) Sygula, A.; Fronczek, F. R.; Sygula, R.; Rabideau, P. W.; Olmstead, M. M. *J. Am. Chem. Soc.* **2007**, *129*, 3842. (e) Diederich, F.; Gómez-López, M. *Chem. Soc. Rev.* **1999**, *28*, 263.

(5) (a) Long, J. R.; Yaghi, O. M. *Chem. Soc. Rev.* **2009**, *38*, 1213and references cited therein. (b) James, S. T. *Chem. Soc. Rev.* **2003**, *32*, 276and references cited therein. (c) Kitagawa, S.; Kitaura, R.; Noro, S.-I. *Angew. Chem., Int. Ed.* **2004**, *43*, 2334. (d) Férey, G. *Chem. Soc. Rev.* **2008**, *37*, 191.

(6) (a) Czaja, A. U.; Trukhan, N.; Müller, U. *Chem. Soc. Rev.* **2009**, *38*, 1284. (b) Düren, T.; Bae, Y.-S.; Snurr, R. Q. *Chem. Soc. Rev.* **2009**, *38*, 1237. (c) Li, J.-R.; Kuppler, R. J.; Zhou, H.-C. *Chem. Soc. Rev.* **2009**, *38*, 1477. (d) Murray, L. J.; Dincă, M.; Long, J. R. *Chem. Soc. Rev.* **2009**, *38*, 1294. (e) Han, S. S.; Mendoza-Cortés, J. L.; Goddard, W. A. *Chem. Soc. Rev.* **2009**, *38*, 1460.

(7) (a) Burrows, A. D.; Frost, C. G.; Mahon, M. F.; Winsper, M.; Richardson, C.; Attfield, J. P.; Rodgers, J. A. *Dalton Trans.* **2008**, 6788. (b) Cavka, J. H.; Jakobsen, S.; Olsbye, U.; Guillou, N.; Lamberti, C.; Bordiga, S.; Lillerud, K. P. *J. Am. Chem. Soc.* **2008**, *130*, 13850. (c) Alkordi, M. H.; Liu, Y.; Larsen, R. W.; Eubank, J. F.; Eddaoudi, M. *J. Am. Chem. Soc.* **2008**, *130*, 12639.

(8) (a) Kurmoo, M. *Chem. Soc. Rev.* **2009**, *38*, 1353. (b) Ma, J.-X.; Huang, X.-F.; Song, X.-Q.; Zhou, L.-Q.; Liu, W.-S. *Inorg. Chim. Acta* **2009**, *362*, 3274. (c) Poulsen, R. S.; Bentien, A.; Chevalier, M.; Iversen, B. B. *J. Am. Chem. Soc.* **2005**, *127*, 9156. (d) Agustí, G.; Muñoz, C. M.; Gaspar, A. B.; Real, J. A. *Inorg. Chem.* **2009**, *48*, 3371. (e) Black, C. A.; Costa, J. S.; Fu, W. T.; Massera, C.; Roubeau, O.; Teat, S. J.; Aromí, G.; Gamez, P.; Reedijk, J. *Inorg. Chem.* **2009**, *48*, 1062.

 Published on Web 11/24/2009

chemistry,[4] and metal-organic frameworks[5] (MOFs). The latter nanoscience consists of organizing metal complexes in multidimensional frameworks while relying on self-assembling organic ligands as linkers.[5a] The most significant advances in the field of MOFs yielded various applications in storage materials,[6] catalysis,[7] magnetic materials,[8] and nanostructures.[9] Another future application of this methodology resides in high-capacity data storage for electronic devices,[10] which can be targeted by the ideal organization of molecular nanomagnets termed single-molecule magnets (SMMs) in a multidimensional environment.[11] Theoretically, such an arrangement of molecular magnets in a crystalline material would enable magnetization probing without the interference of magnetic ordering, allowing researchers to study the exact nature of the retention of the magnetization for SMMs.[12]

A SMM is a discrete molecule that exhibits the superparamagnet-like property of slow relaxation of the magnetization at low temperature.[13] Such behavior is generally observed when the molecule possesses a large spin ground state (S) in combination with a large uniaxial magnetic anisotropy (D), which leads to an anisotropic energy barrier (U). Synthetically speaking, SMMs are commonly isolated using multidentate ligands promoting the formation of large paramagnetic transition metals or lanthanide complexes. The organic ligands not only play an important role in mediating magnetic exchange interactions between metal centers but also are critical in the encapsulation of the inorganic core to prevent intermolecular magnetic interactions.[14] The most employed ligand systems in SMM chemistry are Schiff-base ligands,[15] polyalcohols,[16] carboxylic acid derivatives,[17] and oximate derivatives.[18] Recently, we reported a lanthanide-only SMM with an effective anisotropic barrier (U_{eff}) of 71 K, one of the largest energy barriers reported to date. The latter was synthesized by combining the large intrinsic magnetic anisotropy and the spin ground state of two ferromagnetically coupled Dy^{III} ions using a Schiff-base ligand.[19]

Tetranuclear manganese, iron, cobalt, and nickel complexes with cubane-core topologies have been extensively studied for their unique SMM properties.[20] This geometry sparked our interest due to the single coordination of the carboxylic acid ligand to the tetranuclear core. In addition, as observed in the literature, lanthanides tend to form similar cubane-based structures when reacted with carboxylic acid functionalized ligands.[21]

As part of our research, we are looking toward the adaptation of this synthetic strategy for the supramolecular organization of SMMs in MOFs by reacting lanthanide precursors and carboxylic acid derivatives. The ligand, 4-(4-carboxyphenyl)-1,2,4-triazole (Hcpt) (Scheme 1),[22] was chosen due to: (1) the presence of the asymmetrical coordination sites based on the carboxylic acid and triazolyl functional groups, (2) a rigid backbone, and (3) the possibility of electrostatic interactions with similar moieties, favoring the organization of the molecules on the macromolecular scale. To promote unique topologies in the crystal lattice, the asymmetric ligand was selected following the hard−soft/acid−base

(9) (a) Zhang, F.; Bei, F.-L.; Cao, J.-M.; Wang, X. *J. Solid State Chem.* **2008**, *181*, 143. (b) Su, C.-Y.; Goforth, A. M.; Smith, M. D.; Pellechia, P. J.; Loye, H. C. Z. *J. Am. Chem. Soc.* **2004**, *126*, 3576. (c) Ma, S.; Simmons, J. M.; Yuan, D.; Li, J.-R.; Weng, W.; Liu, D.-J.; Zhou, H.-C. *Chem. Comm.* **2009**, 4049. (d) Kaczorowski, T.; Justyniak, I.; Lipinska, T.; Lipkowski, J.; Lewinski, J. *J. Am. Chem. Soc.* **2009**, *131*, 5393. (e) Dai, F.; He, H.; Sun, D. *J. Am. Chem. Soc.* **2008**, *130*, 14064. (f) Huang, X.-C.; Luo, W.; Shen, Y.-F.; Lin, X.-J.; Li, D. *Chem. Commun.* **2008**, 3995.

(10) (a) Naitabdy, A.; Bucher, J.-P.; Gerbier, P.; Rabu, P.; Drillon, M. *Adv. Mater.* **2005**, *17*, 1612. (b) Leunenberger, M. N.; Loss, D. *Nature* **2001**, *410*, 789.

(11) Roubeau, O.; Clérac, R. *Eur. J. Inorg. Chem.* **2008**, 4325.

(12) Wu, Q.; Li, Y.-G.; Wang, Y.-H.; Clérac, R.; Lu, Y.; Wang, E.-B. *Chem. Commun.* **2009**, 5743.

(13) (a) Christou, G.; Gatteschi, D.; Hendrickson, D. N.; Sessoli, R. *MRS Bull.* **2000**, *25*, 66. (b) Thomas, L.; Lionti, L.; Ballou, R.; Gatteschi, D.; Sessoli, R.; Barbara, B. *Nature* **1996**, *383*, 145. (c) Coronado, E.; Day, P. *Chem. Rev.* **2004**, *104*, 5419. (d) Bogani, L.; Wernsdorfer, W. *Nature Mat.* **2008**, *7*, 179. (e) Sokol, J. J.; Hee, A. G.; Long, J. R. *J. Am. Chem. Soc.* **2002**, *124*, 7656. (f) Maheswaran, S.; Chastanet, G.; Teat, S. J.; Mallah, T.; Sessoli, R.; Wernsdorfer, W.; Winpenny, R. E. P. *Angew. Chem.* **2005**, *44*, 5044. (g) Tang, J.; Hewitt, I.; Madhu, N. T.; Chastanet, G.; Wernsdorfer, W.; Anson, C. E.; Benelli, C.; Sessoli, R.; Powell, A. K. *Angew. Chem.* **2006**, *45*, 1729.

(14) Blundell, S. J. *Contemp. Phys.* **2007**, *48*, 275.

(15) (a) Singh, R.; Banerjee, A.; Colacio, E.; Rajak, K. K. *Inorg. Chem.* **2009**, *48*, 4753. (b) Ababei, R.; Li, Y.-G.; Roubeau, O.; Kalisz, M.; Bréfuel, N.; Coulon, C.; Harté, E.; Liu, X.; Mathonière, C.; Clérac, R. *New J. Chem.* **2009**, *33*, 1237. (c) Hoshino, N.; Ako, A. M.; Powell, A. K.; Oshio, H. *Inorg. Chem.* **2009**, *48*, 3396. (d) Novitchi, G.; Wernsdorfer, W.; Chibotaru, L. F.; Costes, J.-P.; Anson, C. E.; Powell, A. K. *Angew. Chem., Int. Ed.* **2009**, *48*, 1614. (e) Kajiwara, T.; Nakano, M.; Takaishi, S.; Yamashita, M. *Inorg. Chem.* **2008**, *47*, 8604. (f) Miyasaka, H.; Saitoh, A.; Abe, S. *Coord. Chem. Rev.* **2007**, *251*, 2622. (g) Ferbinteanu, M.; Miyasaka, H.; Wernsdorfer, W.; Nakata, K.; Sugiura, K.; Yamashita, M.; Coulon, C.; Clérac, R. *J. Am. Chem. Soc.* **2005**, *127*, 3090. (h) Miyasaka, H.; Clérac, R.; Wernsdorfer, W.; Lecren, L.; Bonhomme, C.; Sugiura, K.-I.; Yamashita, M. *Angew. Chem., Int. Ed.* **2004**, *43*, 2801.

(16) (a) Ferguson, A.; Lawrence, J.; Parkin, A.; Sanchez-Benitez, J.; Kamenev, K. V.; Brechin, E. K.; Wernsdorfer, W.; Hill, S.; Murrie, M. *Dalton Trans.* **2008**, 6409. (b) Murugesu, M.; Raftery, J.; Wernsdorfer, W.; Christou, G.; Brechin, E. K. *Inorg. Chem.* **2004**, *43*, 4203. (c) Stamatatos, T. C.; Poole, K. M.; Abboud, K. A.; Wernsdorfer, W.; O'Brien, T. A.; Christou, G. *Inorg. Chem.* **2008**, *47*, 5006. (d) Stamatatos, T. C.; Nastopoulos, V.; Tasiopoulos, A. J.; Moushi, E. E.; Wernsdorfer, W.; Christou, G.; Perlepes, S. P. *Inorg. Chem.* **2008**, *47*, 10081.

(17) (a) Sessoli, R.; Gatteschi, D.; Caneschi, A.; Novak, M. A. *Nature* **1993**, *365*, 141and references cited therein. (b) Sessoli, R.; Tsai, H.-K.; Schake, A. R.; Wang, S.; Vincent, J. B.; Folting, K.; Gatteschi, D.; Christou, G.; Hendrickson, D. N. *J. Am. Chem. Soc.* **1993**, *115*, 1804. (c) Gatteschi, D.; Sessoli, R. *Angew. Chem., Int. Ed.* **2003**, *42*, 268. (d) Price, D. J.; Batten, S. R.; Moubaraki, B.; Murray, K. S. *Polyhedron* **2007**, *26*, 305.

(18) (a) Papatriantafyllopoulou, C.; Estrader, M.; Efthymiou, C. G.; Dermitzaki, D.; Gkotsis, K.; Terzis, A.; Diaz, C.; Perlepes, S. P. *Polyhedron* **2009**, *28*, 1652. (b) Milios, C. J.; Inglis, R.; Jones, L. F.; Prescimone, A.; Parsons, S.; Wernsdorfer, W.; Brechin, E. K. *Dalton Trans.* **2009**, 2812. (c) Stamatatos, T. C.; Foguet-Albiol, D.; Lee, S.-C.; Stoumpos, C. C.; Raptopoulou, C. P.; Terzis, A.; Wernsdorfer, W.; Hill, S. O.; Perlepes, S. P.; Christou, G. *J. Am. Chem. Soc.* **2007**, *129*, 9484. (d) Mori, F.; Nyui, T.; Ishida, T.; Nogami, T.; Choi, K.-Y.; Nojiri, H. *J. Am. Chem. Soc.* **2006**, *128*, 1440.

(19) Lin, P.-H.; Burchell, T. J.; Clérac, R.; Murugesu, M. *Angew. Chem., Int. Ed.* **2008**, *47*, 8848.

(20) (a) Wernsdorfer, W.; Aliaga-Alcalde, N.; Hendrickson, D. N.; Christou, G. *Nature* **2002**, *416*, 406. (b) Aubin, S. M. J.; Dilley, N. R.; Pardi, L.; Krzystek, J.; Wemple, M. W.; Brunel, L.-C.; Maple, B. M.; Christou, G.; Hendrickson, D. N. *J. Am. Chem. Soc.* **1998**, *120*, 4991. (c) Moubaraki, B.; Murray, K. S.; Hudson, T. A.; Robson, R. *Eur. J. Inorg. Chem.* **2008**, 4525. (d) Feng, P. L.; Beedle, C. C.; Koo, C.; Wernsdorfer, W.; Nakano, M.; Hill, S.; Hendrickson, D. N. *Inorg. Chem.* **2008**, *47*, 3188. (e) Galloway, K. W.; Whyte, A. M.; Wernsdorfer, W.; Sanchez-Benitez, J.; Kamenev, K. V.; Parkin, A.; Peacock, R. D.; Murrie, M. *Inorg. Chem.* **2008**, *47*, 7438. (f) Feng, P. L.; Beedle, C. C.; Wernsdorfer, W.; Koo, C.; Nakano, M.; Hill, S.; Hendrickson, D. N. *Inorg. Chem.* **2007**, *46*, 8126. (g) Oshio, H.; Hoshino, N.; Ito, T. *J. Am. Chem. Soc.* **2000**, *122*, 12602. (h) Aliaga-Alcalde, N.; Edwards, R. S.; Hill, S. O.; Wernsdorfer, W.; Folting, K.; Christou, G. *J. Am. Chem. Soc.* **2004**, *126*, 12503. (i) Aubin, S. M. J.; Wemple, M. W.; Adams, D. M.; Tsai, H.-L.; Christou, G.; Hendrickson, D. N. *J. Am. Chem. Soc.* **1996**, *118*, 7746.

(21) (a) Ma, B.-Q.; Zhang, D.-S.; Gao, S.; Jin, T.-Z.; Yan, C.-H.; Xu, G.-X. *Angew. Chem., Int. Ed.* **2000**, *39*, 3644. (b) Kajiwara, T.; Iki, N.; Yamashita, M. *Coord. Chem. Rev.* **2007**, *251*, 1734. (c) Zheng, X.-J.; Jin, L.-P.; Gao, S. *Inorg. Chem.* **2004**, *43*, 1600. (d) Wang, R.; Selby, H. D.; Liu, H.; Carducci, M. D.; Jin, T.; Zheng, Z.; Anthis, J. W.; Staples, R. J. *Inorg. Chem.* **2002**, *41*, 278.

(22) (a) Bayer, H. O.; Cook, R. S.; Meyer, W. C. V. US Patent 3,821,376, **1974**.(b) Zou, R.-Q.; Cai, L.-Z.; Guo, G.-C. *J. Mol. Struct.* **2005**, *737*, 125. (c) Lukashuk, L. V.; Lysenko, A. B.; Rusanov, E. B.; Chernega, A. N.; Domasevitch, K. V. *Acta Crystallogr., Sect. C: Cryst. Struct. Commun.* **2007**, *C63*, m140.

Scheme 1. Representation of the 4-(4-carboxyphenyl)-1,2,4-triazole (Hcpt) Ligand

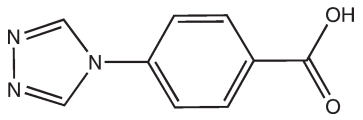

concept; hard lanthanide ions favor the coordination of acidic carboxylic acids over the coordination of basic nitrogen-based functional groups.[23] Furthermore, we believe that the weak-coordinating triazole group will in turn participate in the arrangement of the molecular units in a multidimensional environment.

Herein, we report the preparation, the structural description, and the magnetic properties of an octanuclear cubane-shaped dumbbell SMM, $[Dy^{III}_4(\mu_3-OH)_2(\mu_3-O)_2(cpt)_6(MeOH)_6(H_2O)]_2$ (**1**·15MeOH), where cpt = 4-(4-carboxyphenyl)-1,2,4-triazole, and analogous Ho^{III} (**2**·14MeOH), and Tb^{III} (**3**·18MeOH) complexes.

Experimental Section

General. All reagents were purchased from either Sigma-Aldrich or Strem chemicals and used without further purification.

Ligand Synthesis. The Hcpt ligand was synthesized according to a modified known procedure.[1a] The intermediate, *N*,*N*′-diformylhydrazine, was synthesized by heating an ethanolic solution (20 mL) of *N*-formylhydrazine (0.45 g, 7.5 mmol) and triethylorthoformate (TEOF) (1.87 mL, 11.3 mmol) at 180 °C for 5 min in a Biotage Initiator 60 microwave apparatus. To generate Hcpt, solid 4-aminobenzoic acid (PABA) (1.0 g, 7.5 mmol) was added to the solution, and the mixture was heated again at 180 °C at 9 bar of pressure for 5 min with vigorous stirring. As the temperature decreased, the ligand precipitated as a pale-yellow powder, which was centrifuged for 15 min at 3 000 rpm and dried in vacuo for 1 h. Recrystallization of the ligand was carried out by dissolving the bulk pale-yellow powder in 45 mL of *N*,*N*′-dimethylformamide (DMF) at 120 °C for 30 min. The solution was then cooled to 40 °C, and 10 mL of diethyl ether was slowly added to the mixture. The precipitated pale-yellow powder was filtered, and colorless needles were obtained from the filtrate after one week without disturbance. Yield = 0.78 g, 55%. ^{1}H NMR (DMSO-d^6, 400 MHz): 13.19 (s, 1H), 9.20 (s, 2H), 8.06 (d, 2H), 7.85 (d, 2H). IR (Hcpt, KBr, cm^{-1}): 3 462 (br), 3 026 (br), 2 793 (s), 2 501 (br), 1 898 (m), 1 696 (m), 1 607 (m), 1 529 (m), 1 451 (m), 1 373 (s), 1 307 (br), 1 249 (s), 1 214 (s), 1 183 (s), 1 082 (s), 1 016 (s), 868 (s), 771 (s), and 694(s).

Crystal data for Hcpt·DMF ($C_{12}H_{16}N_4O_3$): M_r = 264.29; triclinic; space group: *P*-1; a = 3.917(1), b = 10.563(4), and c = 15.144(6) Å; α = 81.941(5)°; β = 89.277(9)°; γ = 87.82(1)°; V = 619.9(4) Å^3; Z = 2; D_c = 1.416 g/cm^3; and R = 0.0859, wR_2 = 0.1477.

Synthesis of Ln^{III} Complexes. The complexes, $[Ln^{III}_4(\mu_3-OH)_2(\mu_3-O)_2(cpt)_6(MeOH)_6(H_2O)]_2$ (Ln = Dy (**1**·15MeOH), Ho (**2**·14MeOH), and Tb (**3**·18MeOH)), were prepared by slowly adding a solution of NaN_3 (0.016 g, 0.50 mmol) and Hcpt (0.024 g, 0.25 mmol) in DMF (2 mL) and MeOH (3 mL) to a solution of $LnCl_3 \cdot 6H_2O$ (0.25 mmol, Ln = Dy (**1**), Ho (**2**), and Tb (**3**)) in MeOH (25 mL). The mixture was stirred for 15 min at room temperature and then filtered. The filtrate was left undisturbed for several days to provide plate-like crystals suitable for single-crystal X-ray diffraction. Yields = 0.109 g (**1**, 76.0%), 0.019 g (**2**, 13.1%), and 0.034 g (**3**, 23.3%).

IR (**1**, KBr, cm^{-1}): 3 451 (br), 1 641 (m), 1 600 (m), 1 563 (m), 1 522 (m), 1 409 (m), 1 375 (s), 1 310 (s), 1 243 (s), 1 109 (s), 1 093 (s), 865 (s), 777 (s), 689 (s).

IR (**2**, KBr, cm^{-1}): 3 441 (br), 1 651 (m), 1 605 (m), 1 563 (m), 1 528 (m), 1 413 (m), 1 384 (s), 1 307 (s), 1 244 (s), 1 091 (s), 1 006 (s), 865 (s), 789 (s), 699 (s).

IR (**3**, KBr, cm^{-1}): 3 436 (br), 1 651 (m), 1 605 (m), 1 563 (m), 1 532 (m), 1 413 (m), 1 310 (s), 1 377 (s), 1 243 (s), 1 093 (s), 1 005 (s), 865 (s), 787 (s), 705 (s).

Crystal data for **1**·15MeOH, ($C_{135}H_{188}Dy_8N_{36}O_{61}$): M_r = 4591.21; triclinic; space group: *P*-1; a = 16.446(4), b = 16.476(4), c = 19.793(5) Å; α = 91.545(4)°; β = 96.707(4)°; γ = 101.977(4)°; V = 5203(2) Å^3; Z = 1; D_c = 1.465 g/cm^3; and R = 0.0813, wR_2 = 0.2487.

IR and NMR Spectroscopy. Infrared analyses (Supporting Information) were obtained using a Nicolet Nexus 550 FT-IR spectrometer in the 4 000−650 cm^{-1} range. The spectra were recorded in the solid state by preparing KBr pellets. NMR analyses were conducted on a Bruker Avance 400 spectrometer equipped with an automatic sample holder and a 5 mm auto-tuning broadband probe with Z gradient.

Single-Crystal X-ray Diffraction Studies. Colorless plate-like crystals of **1** suitable for single-crystal X-ray diffraction were mounted on a glass fiber. Unit cell measurements and intensity data collections were performed on a Bruker-AXS SMART 1 k CCD diffractometer using graphite monochromated MoK_α radiation (λ = 0.71073 Å). The data reduction included a correction for Lorentz and polarization effects, with an applied multiscan absorption correction (SADABS). The interatomic distances and angles are listed in the Supporting Information, Table S1. The reflection data were consistent with a triclinic system *P*-1. The crystal structure was solved and refined using the SHELXTL program suite. In all cases, the crystals diffracted weakly. For **1**, the data were truncated at 23.26°. Direct methods yielded non-hydrogen atoms. The hydrogen atoms of the coordinated water molecules could not be located from the difference Fourier maps; they are, therefore, included in the chemical formula but absent from the res and cif files, creating a discrepancy in the cifcheck file. All other hydrogen atom positions were calculated geometrically and were riding on their respective atoms. Some of the methanol solvent molecules of crystallization were disordered and were modeled at either 50% occupancy or over two positions as a 50:50 isotropic mixture with light restraints. The largest residual electron density peaks (2.550 e$^-$/Å^3) were associated with the Ln1 atom. Full-matrix least-squares refinement on F^2 gave R_1 = 0.0813 and wR_2 = 0.2487 at convergence. For complexes **2** and **3**, unit cell measurements and intensity data collections were carried out. From the collected data, the molecular structure and the connectivity were obtained, which confirmed that the complexes were isomorphous. However, due to the poor diffraction of the crystals, both structures could not be refined with acceptable R_1 factors.

Magnetic Measurements. The magnetic susceptibility measurements were obtained using a Quantum Design SQUID magnetometer MPMS-XL operating between 1.8 and 300 K for dc-applied fields ranging from −7 to 7 T. Dc analyses were performed on polycrystalline samples of 6.6, 5.1, and 5.5 mg of **1**, **2**, and **3**, respectively, wrapped in a polyethylene membrane and under a field ranging from 0 to 7 T between 1.8 and 300 K. Ac susceptibility measurements were carried out under an oscillating ac field of 3 Oe and ac frequencies ranging from 1 to 1 500 Hz. The magnetization data were collected at 100 K to check for ferromagnetic impurities that were absent in all samples. A diamagnetic correction was applied for the sample holder.

Results and Discussion

Preparation of the Ligand. The Hcpt ligand was prepared following a modified known procedure.[1a] The

(23) Gu, X.; Xue, D.; Ratajczak, H. *J. Mol. Struct.* **2008**, *887*, 56and references cited therein.

Scheme 2. Preparation of the Hcpt Ligand

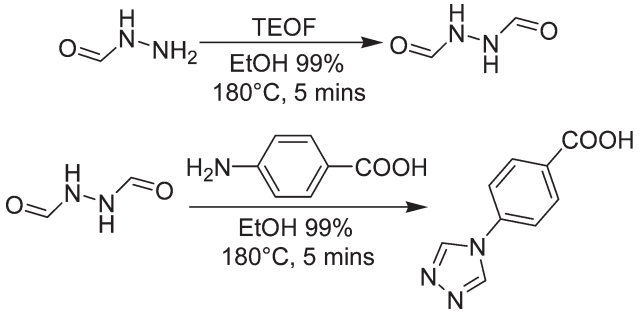

reaction (Scheme 2) was performed as a two-step synthesis in a Biotage Initiator 60 microwave apparatus. By means of the method described previously,[1a] the same compound was obtained in a much lower yield. For the synthesis of a larger amount of the ligand, high-pressure glass vessels were employed instead of the microwave apparatus, which resulted in a slightly lower yield for the overall procedure. Recrystallization of the ligand was performed not only to purify the ligand but also to obtain a better insight on the structural properties of the neutral ligand. The crystallographic data were obtained by analyzing the colorless needle-like crystals using single-crystal X-ray diffraction (two-dimensional (2D) Figure S1, Supporting Information).

Preparation of the Complexes. A useful synthetic procedure that has been employed in the preparation of polynuclear lanthanide aggregates is the reaction of carboxylate ligands with lanthanide precursors.[19] Such reactions in basic conditions foster the formation of oxy/hydroxy cluster complexes where the central core is encapsulated by carboxylate groups. With this in mind, we have explored the reaction of the Hcpt ligand with various lanthanide precursors. The treatment of lanthanide trichloride hydrates with Hcpt in presence of NaN_3 in a 2:1:2 molar ratio in 25 mL of a 5:1 mixture of methanol and DMF yielded the $\{Ln^{III}{}_4\}_2$ (**1**, **2**, and **3**) complexes. The formation of those complexes is summarized in eq 1:

$$12\text{Hcpt} + 8\text{LnCl}_3\cdot 6\text{H}_2\text{O} \xrightarrow[\text{MeOH/DMF}]{} [\text{Ln}^{\text{III}}{}_4(\mu_3\text{–OH})_2(\mu_3\text{–O})_2(\text{cpt})_6(\text{MeOH})_6(\text{H}_2\text{O})]_2\cdot(x\text{MeOH}) \quad (1)$$

The sodium azide employed reaction procedure does not participate in the coordination of the $\{Ln^{III}{}_4\}_2$ complexes. However, the azide anion plays an important role as a mild base by promoting the deprotonation of the Hcpt ligand. When stronger bases, such as sodium hydroxide and triethylamine, were employed, fluffy white or pale-pink powders of the $\{Ln^{III}{}_4\}_2$ complexes were obtained instead of a crystalline material. Using an exact ligand-to-metal ratio of 4:3, as described in eq 1, instead of a 2:1 ratio also resulted in white or pale-pink powders of the complexes. In addition, DMF was used as a cosolvent in the reaction mixture to increase the solubility of the ligand and to promote slow crystallization. In the absence of DMF, all three complexes precipitated in a powdered form in a short period of time.

Structural Analyses. The dimeric molecular structure of **1**, $\{Dy^{III}{}_4\}_2$, is shown in Figure 1, and a fully labeled view

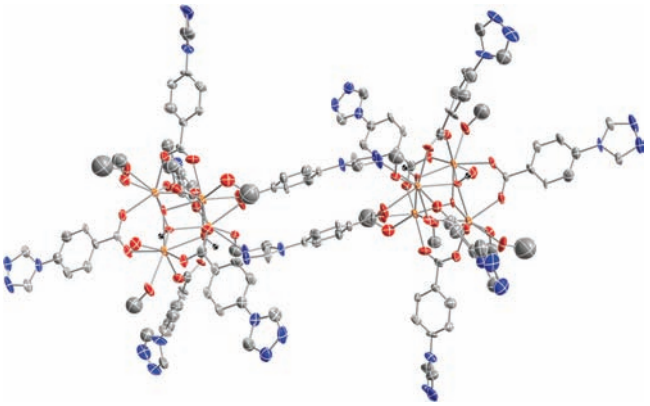

Figure 1. Molecular structure of $[Dy^{III}{}_4(\mu_3\text{–OH})_2(\mu_3\text{–O})_2(\text{cpt})_6(\text{MeOH})_6(\text{H}_2\text{O})]_2$, **1**. Thermal ellipsoids are set at 50% probability. The hydrogen atoms and the solvent molecules are omitted for clarity. Color code: orange (Dy^{III}), red (O), blue (N), gray (C), and black (H).

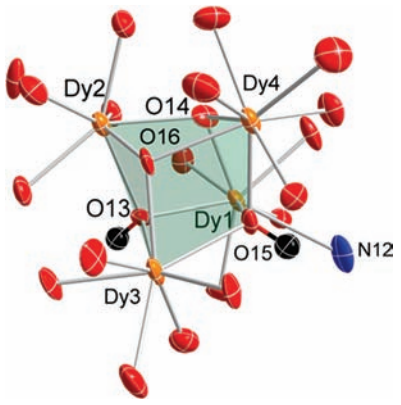

Figure 2. Ellipsoidal representation of the cubane core of **1** at 50% probability. Color code: orange (Dy^{III}), red (O), blue (N), and black (H).

of the central $\{Dy^{III}{}_4\}$ core of the molecule is shown in Figure 2. By analyzing the connectivity of the atoms from the collected crystallographic data for **2** and **3**, both complexes were proven to be isomorphous to **1**. The selected bond distances and angles for **1** are available in Table 1. The overall dumbbell-shaped dimeric structure is composed of two cubane moieties, $\{Dy^{III}{}_4(\mu_3\text{–O})_2(\mu_3\text{–OH})_2\}^{6+}$, where each unit is encapsulated by carboxylate groups from six cpt^- ligands. Two of the ligands link the two cubane units to form the dimeric dumbbell-shaped complex. The $\{Dy^{III}{}_4(\mu_3\text{–O})_2(\mu_3\text{–OH})_2\}^{6+}$ core of **1** (Figure 2) is composed of four Dy^{III} ions linked by four μ_3 oxy/hydroxy moieties. On average, the bond distances between the O13 and O15 and their respective Dy^{III} atoms, except between Dy1 and O15, are about 2.40(2) Å, while the distances between the O14 and O16 and the metal centers are approximately 2.35(2) Å. This difference in the coordination bond lengths, along with charge consideration, indicates that the cubane moiety is most likely to be composed of two μ_3-hydroxides (O13 and O15) and two μ_3-oxides (O14 and O16), which cause an asymmetrical distortion of the core.

On each Dy^{III} ion, three other coordination sites are occupied by anionic ligands, while the remaining sites are connected either to solvent molecules or, in the case of Dy1, to a triazole nitrogen atom from a neighboring $\{Dy^{III}{}_4\}$ molecule. By considering the different natures

Table 1. Selected Bond Distances and Angles of **1**

Bond Distances (Å)			
Dy1−O15	2.31(1)	Dy3−O16	2.36(1)
Dy1−O14	2.35(1)	Dy3−O15	2.40(1)
Dy1−O13	2.41(1)	Dy3−O13	2.39(1)
Dy1−N12	2.77(2)	Dy4−O15	2.41(1)
Dy2−O14	2.37(1)	Dy4−O16	2.34(1)
Dy2−O13	2.36(1)	Dy4−O14	2.39(1)
Dy2−O16	2.33(1)		
Angles (°)			
Dy1−O13−Dy2	107.3(4)	Dy2−O13−Dy3	104.5(4)
Dy1−O14−Dy2	108.9(5)	Dy2−O16−Dy3	106.4(5)
Dy1−O15−Dy3	107.8(4)	Dy2−O14−Dy4	103.7(4)
Dy1−O13−Dy3	105.1(4)	Dy2−O16−Dy4	106.6(5)
Dy1−O15−Dy4	105.8(4)	Dy3−O15−Dy4	103.9(4)
Dy1−O14−Dy4	104.8(4)	Dy3−O16−Dy4	107.4(5)

of the bridging μ_3-agents, the presence of six anionic ligands in the structure, and the absence of counteranions in the crystal lattice, the oxidation state of each lanthanide ion was considered to be +3.

As aforementioned, the Dy2, Dy3, and Dy4 ions are octacoordinated to three μ_3-O^{2-} or μ_3-OH^-, three anionic ligands, and two MeOH and/or H_2O molecules. On the other hand, the coordination of the external triazole functional group, from the neighboring molecule, to Dy1 forms the dumbbell-shaped $\{Dy^{III}_4\}_2$ molecule (Figure 1). The bridge is composed of two parallel ligands coordinated to either one of the Dy1 atoms through the triazole nitrogen atoms. The bond distance between these atoms is 2.77(2) Å, suggesting a weak nitrogen-based coordination bond strength. The presence of this external coordination is supported by the fact that the bridging ligand has a torsion angle of ~ 45.6°, which is larger than the free ligand's torsion angle of ~ 33.5° (Supporting Information, Figure S2). The packing arrangement of **1** (Figure 3 and S4 and S5, Supporting Information) is composed of $\{Dy^{III}_4\}_2$ moieties organized in a 2D sheet through interactions of their equatorial ligands.

The coordination of the carboxylate functional group to the Dy^{III} ions decreases the electron density located at the COO^- end of the ligand, while the triazole aromatic rings are electron-rich functional groups due to the delocalization of the π-nitrogen electrons in the aromatic system. These facts led us to the conclusion that the ligands are electrostatically interacting between the electron-rich triazole aromatic ring and the electron-deficient coordinated carboxylate functional group, which results in the observed 2D organization of the molecules analogous to MOFs. For **1**, each quadrilateral space between the constituents is occupied by four methanol molecules and two axial sheets' ligands (Supporting Information, Figure S6). The distances between the corners of these spaces and their angles are described in Scheme 3.

Magnetic Properties. The dc magnetic measurements were performed on polycrystalline samples of **1**, **2**, and **3** between 1.8 and 300 K under an external field of 1 000 Oe (Figure 4, top). At room temperature, the χT product values are 55.7, 54.2, and 46.5 cm^3 K mol^{-1} for **1**, **2**, and **3**, respectively. These values are close to the expected Curie

(24) Benelli, C.; Gatteschi, D. *Chem. Rev.* **2002**, *102*, 2369.

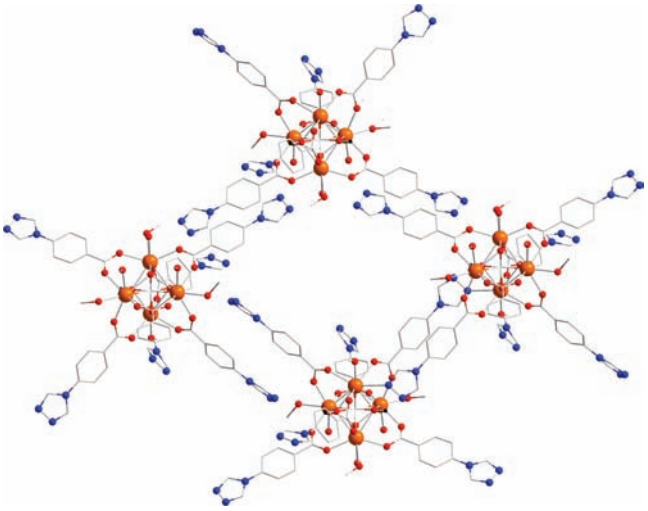

Figure 3. The packing diagram of **1** in the (*ab*) plane. The hydrogen atoms, except for the core hydrogen atoms, and the solvent molecules are omitted for clarity. Color code: orange (Dy^{III}), red (O), blue (N), gray (C), and black (H).

Scheme 3. Drawing of the Quadrilateral Space between The $\{Dy^{III}_4\}_2$ Dumbbell Units in the Crystal Lattice[a]

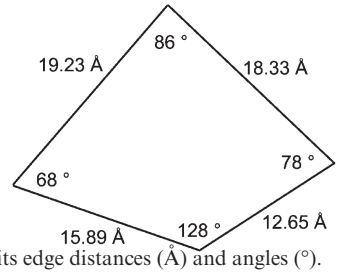

[a] Describing its edge distances (Å) and angles (°).

constants[24] for four noninteracting free Ln^{III} ions; Dy^{III}: 56.7 cm^3 K mol^{-1} (S = 5/2, L = 5, g = 4/3, and C = 14.17 cm^3 K mol^{-1}), Ho^{III}: 56.3 cm^3 K mol^{-1} (S = 2, L = 6, g = 5/4, and C = 14.08 cm^3 K mol^{-1}), and Tb^{III}: 47.3 cm^3 K mol^{-1} (S = 3, L = 3, g = 3/2, and C = 11.82 cm^3 K mol^{-1}). Upon cooling, the χT product slowly decreases to reach the minimal values of 33.1, 17.9, and 26.8 cm^3 K mol^{-1} at 1.8 K. The declining χT product can be explained by three factors: (i) antiferromagnetic interactions between the lanthanide ions of the cubane core, (ii) depopulation of the ground-state Ln^{III} sublevels that result from a spin−orbit coupling and a low-symmetry crystal field, or (iii) magnetic anisotropy. Due to the presence of all these combined effects in these tetranuclear complexes, it is difficult to quantify separately each contributions.

For all three complexes, the temperature dependence of the magnetization between 1.8 and 8 K reveals an absence of saturation under large dc-applied fields (Figure 4, bottom for **1** and Supporting Information, Figure S1 for **2** and **3**). For **1**, at 1.8 K and above 1 T, the magnetization increases slowly without reaching saturation up to 22.7 μ_β under a field of 7 T. In agreement with the χT vs. T data described above, this lack of saturation is indicative of magnetic anisotropy and/or of a field-induced population of the low-lying excited states. For **2** and **3**, the magnetizations quickly increase below 1 T then slowly augment up to the unsaturated values of 22.8 and

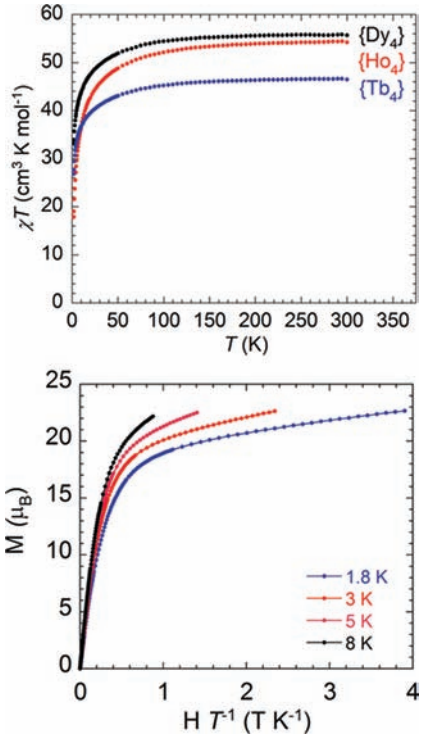

Figure 4. Top: dc susceptibility of **1** (black), **2** (red), and **3** (blue) from 1.8 to 300 K under an external dc-applied field of 1 000 Oe. Bottom: temperature dependence of the magnetization of **1** measured at 1.8, 3, 5, and 8 K.

19.8 μ_β, respectively, at 1.8 K under a field of 7 T (Supporting Information, Figure S1).

Temperature dependences of the ac susceptibility were measured for all three complexes under an ac field of 3 Oe oscillating with frequencies ranging between 10 and 1 500 Hz. For **2** and **3**, no noticeable out-of-phase susceptibility is observed above 1.8 K. For **1** (Figure 5), upon cooling, the frequency-dependent increase of the out-of-phase component of the ac susceptibility (χ"), up to a maximum value of 1.50 cm^3 mol^{-1} at 1 500 Hz and 1.8 K, suggests the presence of a slow relaxation of the magnetization, which might be the signature of a SMM behavior.

In order to further probe the behavior of **1**, field dependence of magnetization measurements were carried out on a single crystal of **1** between 0.04 and 7 K and under dc-applied fields ranging from −1.4 to 1.4 T on a micro-SQUID apparatus.[25] The measurements, performed by applying the magnetic field along the magnetic easy axis of the crystal, reveal that **1** exhibits a small M/M_S vs H hysteresis loop even at 0.04 K (Figure 6). The sweep-rate dependency of the hysteresis loop (Figure 7) confirms that **1** exhibits a slow relaxation of magnetization that is characteristic of SMMs. The large separation between the octanuclear $\{Dy^{III}{}_4\}_2$ units, seen in the crystal lattice of **1**, points to an absence of significant intermolecular magnetic interactions and, thus, supports the SMM behavior. The occurrence of a step-like feature in the hysteresis loop indicates either quantum tunneling of the magnetization (QTM), as usually observed for polynuclear systems, or individual reversal of magnetization of each Dy^{III} ion.[13] For such polynuclear lanthanide

(25) Wernsdorfer, W. *Adv. Chem. Phys.* **2001**, *118*, 99.

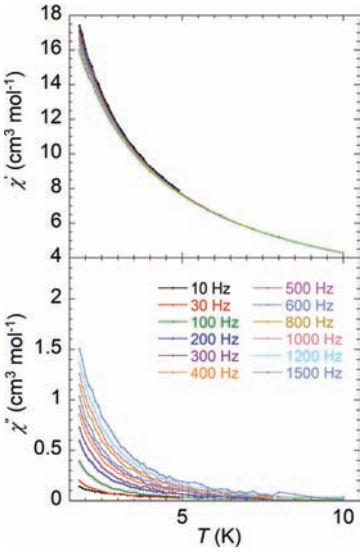

Figure 5. Temperature dependence of the in-phase (χ', top) and out-of-phase (χ", bottom) components of the ac susceptibility of **1** using frequencies between 10 and 1 500 Hz.

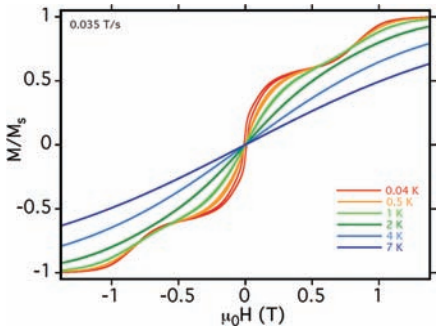

Figure 6. Field dependence of the normalized magnetization of **1** between 0.04 and 7 K under dc-applied fields ranging from −1.5 to 1.5 T, where M_S is the magnetization at saturation.

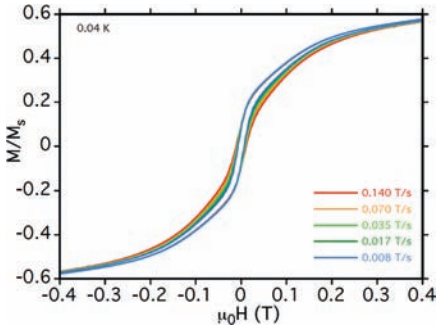

Figure 7. Field sweep-rate dependence of the M/M_S vs H hysteresis loop for **1** at 0.04 K.

systems, the shape/positioning of the steps usually originates from the weak exchange interactions and also depends on the orientation of the applied field in relation to the anisotropic plane of the molecule.[13g] Ab inito calculations are currently underway to elucidate the anisotropic plane of the molecule as well as the in-depth analysis of the steps. The small coercivity of the hysteresis loop and the presence of ac signal only at low temperatures suggest a small effective barrier (U_{eff}) for **1**. This

might be due to the commonly occurring fast QTM in lanthanide systems.

Conclusion

A lanthanide-only cubane-shaped dumbbell single-molecule magnets (SMMs), $[Dy^{III}_4(\mu_3-OH)_2(\mu_3-O)_2(cpt)_6(MeOH)_6(H_2O)]_2\cdot(15MeOH)$ (**1**), and its Ho^{III} (**2**) and Tb^{III} (**3**) analogues were prepared, structurally analyzed, and magnetically characterized. The complexes were designed by choosing a ligand, Hcpt that favors the synthesis of such molecules. The structural analyses demonstrated that the $\{Dy^{III}_4\}_2$ cubane-shaped dumbbell moieties are organized in a topology analogous to a two-dimensional (2D) metal-organic framework (MOF) environment that emerges from the electrostatic interactions of the ligands. To date, only a few lanthanide-only cubane-shaped structures have been prepared by using alkylated carboxylic acid derivatives as ligands, preventing the structural rigidity needed to organize the molecules in the crystal lattice. Moreover, the large span between the $\{Dy^{III}_4\}_2$ species in the crystal lattice suggested the absence of magnetic interactions between the units. This was confirmed by asserting the magnetic properties of **1**, which also indicated that the complex behaves as a lanthanide-only cubane-shaped SMM with a small energy barrier. To our knowledge, **1** is the first cubane-shaped lanthanide-only molecule that exhibits slow relaxation of magnetization. Since the previously published undistorted lanthanide-only cubane-shaped structures did not exhibit slow relaxation of magnetization, the distortion of the cubane core might be at the origin of this fascinating property. In order to confirm this assumption, our current work focuses on accentuating the deformation of the core by substituting functional groups on the Hcpt ligand and by replacing the solvent molecules coordinated to the cubane-shaped core.

Acknowledgment. We thank the University of Ottawa, the Canada Foundation for Innovation (CFI), FFCR, NSERC (Discovery and RTI grants), the University of Bordeaux, the CNRS, and the "Région Aquitaine" for financial support.

Supporting Information Available: The reduced magnetization plots of **2** and **3**, the molecular structure of 4-(4-carboxyphenyl)-1,2,4-triazole (Hcpt), the infrared spectroscopy discussion, the IR spectra of **1**, **2**, and **3**, the packing arrangement of **1** viewed along the (*ab*) plane, the packing arrangement of **1** viewed along the *c*-axis, and the packing diagram of two superimposed sheets of **1** viewed along the (*ab*) plane. This material is available free of charge via the Internet at http://pubs.acs.org.